Int J Adv Manuf Technol (2017) 92:4199–4211
DOI 10.1007/s00170-017-0481-0

ORIGINAL ARTICLE

Experimental characterisation and modelling of rheokinetic properties of different silicone elastomers

H. Ou[1] · **M. Sahli**[1] · **T. Barriere**[1,2] · **J. C. Gelin**[1]

Received: 22 August 2016 / Accepted: 28 April 2017 / Published online: 13 May 2017

Abstract Elastomer injection moulding is a process whereby an elastomer mix is injected into a closed mould where the material is shaped to the desired geometry. Once completely filled, the silicone elastomer mix is vulcanised. Vulcanisation is the process whereby a viscous flow of silicone is converted into an elastic material through the incorporation of chemical cross-links between the material chains. To correctly use simulation tools to predict the filling of die mould cavities, it is necessary to characterise the material in terms of their rheological properties and kinetic behaviour during curing. The aim of this study was to develop mathematical models for the thermo-kinetic parameters of elastomers that can properly predict the filling of the die mould cavity. In this work, a rotational rheometer was used to determine changing viscosity and vulcanisation characteristics of a silicone compound. The rheokinetic properties of different silicone fluid samples were measured over a broad temperature range from 25 to 100 °C and are reported in this paper. Good agreement was obtained between the experimental results and the model predictions. The methods proposed could well represent the overall experimental data for different silicone elastomers; thus, it could be readily employed for simulation of the elastomer injection moulding process.

Keywords Silicone · Viscosity · Vulcanisation · Kinetic modelling · Parameter identification · Simulation

Highlights - The rheological and kinetic properties of different materials were compared.
- The rheokinetic models for elastomer silicones were investigated.
- An inverse modelling approach for the rheokinetic identification of elastomeric silicones was used.
- The experimental results compare favourably with theoretical predictions without causing a significant difference.
- Simulation of elastomer injection moulding process has been investigated.

✉ T. Barriere
thierry.barriere@ens2m.fr

[1] Femto-ST Institute, Department of Applied Mechanics, University Bourgogne-Franche-Comté, COMUE UBFC, 24 Rue de l'Epitaphe, 25030 Besançon, France

[2] University of Franche-Comté, 26 Chemin de l'Epitaphe, 25000 Besançon, France

1 Introduction

Silicone elastomers are a specific category of elastomeric materials that have many interesting physical and chemical properties, such as good thermal, chemical and mechanical stabilities; good biocompatibility; and high elasticity. Injection moulding of elastomers for large-scale production components, such in the automotive and biomedical industries, is a critical manufacturing process. Today, silicone elastomers are used in many industries because of their stable and high-performance properties and are used as wire sealants and engine gasketing in aerospace applications, safety cables and insulators in electronic applications and tube and respiration masks in medical applications [1]. In addition, room temperature vulcanizing (RTV) silicone elastomers are widely used for producing replicas in industry and in the laboratory due to the easy manufacturing process through the use of vacuum casting 2D die cavity micromoulds to produce elaborate microgear components [2] or helicoidal gear shape components [3]. It is important to have a high-quality mould casting to obtain a very accurate replication. Sahli and al. developed a novel process by hot embossing process with high loaded polymer using elastomeric replica mould [4]. That is used to replicate polymer microfluidic chips whilst simultaneously

reducing the channel surface roughness of the mould insert, yielding optical-grade (less than 100-nm surface roughness) channels and reservoirs. The limit of a line width replication of approximately 40 nm has been successfully obtained using the vacuum casting process [5]. Actually, the size of the micromoulds is smallest for soft lithographic processes that are currently used in different fields ranging from microelectronics to biology [6, 7]. L. bernardi et al. have performed the cyclic deformation behaviour, fracture properties and cytotoxicity with some silicone-based elastomers used as substrates for mechanobiological studies or in soft biomedical implants such as skin-like applications or external maxillofacial prosthetics [8].

The casting process of a RTV silicone elastomer generally consists of four stages: mixing elastomer components A and B at a specific weight ratio, degassing the mixture for the first time to eliminate trapped air bubbles, pouring the mixture into the mould and evacuating a second time, curing the mixture at a given temperature using an oven and obtaining the silicone elastomer components by demoulding. In addition, the cure kinetics of silicone elastomers depend upon several factors, of which the most important are believed to be the composition of the silicone elastomer, the test temperature and the method, used to characterise the material [9]. The vulcanisation process has a crucial influence on the performance and quality of the final silicone elastomer product. A suitable vulcanisation process can improve the properties of silicone elastomers, such as the tear strength, elongation at break, hardness and compression modulus. The current methods to describe the curing of a silicone elastomer material are differential scanning calorimetry (DSC), an oscillating disc rheometer (ODR) and a moving die rheometer (MDR) [10]. In DSC measurements, the cure degree is related to the heat released during the cross-linking reaction. Otherwise, in an ODR measurement, the cure degree is attached to the evolution of the elastic modulus.

Polgar et al. investigated the cross-linking conversions obtained from spectroscopic methods with Fourier transform infrared spectroscopy [11]. The differences in relative peak areas were used to determine the reaction conversions. There observed that the deviation between the concentration of cross-links as determined by infrared spectroscopic analysis and rheology methods confirmed that the former also measures the formation of the initial Diels-Alder adduct, whereas the latter only determines the formed cross-links.

From such different methods, a parameter known as the cure degree is defined and plotted versus time to provide a useful representation to describe the temporal behaviour of the curing reaction [12]. Many models have been proposed to describe the curing process. Two types of system models have been developed in the literature: kinetic models [13] and phenomenological or empirical models [14]. Kinetic models have been used to relate the rate and cure degree and describe the chemical reactions that occur during the curing process. This type of model quantifies the balance of the chemical species involved in the reactions to form the mathematical relationships connecting the reaction rate path to the cure time and temperature. M.R. Erfanian et al. investigated the optimum curing time for thick moulded rubber components [15]. There works are focused on the computational modelling for numerical simulation of the vulcanisation in injection moulding process. There proposed a method for determining the optimal curing time in the three-dimensional complex component. Their main innovation is to propose a kinetic model with variable order of reaction, which enhances the accuracy of the calculated optimal curing time.

Many kinetic models have been developed to describe the cure behaviour [16] especially with the models of Kamal and al. [17] and Isayev and al. [18]. The Deng Isayev, Setak-Berggren and Kamal models are members of a hierarchy of increasing complexity. In-Kwon H. et al. investigated the kinetics of the cross-linking reaction of polydimethylsiloxane (PDMS) [19]. The kinetic parameters of the reaction were determined with different conventional kinetic model as the Kissinger, the Ozawa, the Flynn-Wall-Ozawa and the Friedman methods. The processing time and temperature of the PDMS were predicted by the direct integration of the modified autocatalytic model with the data from isothermal runs and give a valuable guide for the thermal processing.

For controlling and assuring quality during the manufacture of silicone elastomer components, an investigation was performed to experimentally characterise and numerically simulate the rheokinetic models of four RTV silicone elastomers in this paper. Four commonly RTVs used were selected to cover a range of mechanical characteristics representative of the materials used for biomedical devices [7, 8] or using elastomeric replica mould [4]. The aim of this study was to measure the shear viscosity and curing behaviours of the elastomer materials at shear rates and temperatures typically encountered in the casting process of RTV silicone elastomers and to evaluate the predictive capability of the conventional viscosity model and cure kinetic model. Deng-Isayev model is able to describe very well the experimental vulcanisation characteristic data of all studied compounds during the fitting process [13, 20] and was used to determine the cure behaviour.

In recent years, there has been increasing demand for simulation-driven designs, which will reduce the cost and time required for product development by using different software packages (Cadmould©, MPI Moldflow©, etc.) to avoid mould filling defects and to optimise the injection parameters [21].

The identification of different rheokinetic models using different RTV elastomer silicones through the inverse modelling approach resulted in a material database, and this database was implemented in the moulding simulation Cadmould® 3D software that was used for the detailed design of the injection moulding process to obtain the mould filling state and cure degree evolution.

The rheological measurements were carried out using a rotational HAAKE MARS III rheometer with a cone-and-plate geometry with an angle of 2°. The experimental rheological results were fitted using both the power-law model and the Carreau-Yasuda model, and the temperature dependence was described using the Arrhenius equation. The curing measurements were also carried out using the rotational HAAKE MARS III rheometer but with a plate-and-plate geometry and in a dynamic mode. In this study, the Deng-Isayev model was utilised to fit the experimental curing curve, and the induction period was characterised using the Claxon-Liska model.

2 Materials and experimental techniques

2.1 Materials

Commercially, RTV silicone elastomers provided by Wacker ELASTOSIL® were used in this study. They cure at room temperature and are ideal for bonding, sealing or encapsulation. The mechanical properties of the different RTV silicone elastomers used in this study and their characteristic are shown in detail in Table 1. The preparation of the elastomers analysed in this study is summarised in Table 1. RTV silicone elastomers are room temperature vulcanised with a two-component silicone elastomer of base polymer (part A) and cross-linker (part B). These two components are not reactive alone; once mixed, they produce a cross-linking reaction. In the case of the M4641 and M4670, the 10:1 ratio is widely used for mechanobiology studies (e.g. ref. [7, 8]) and was adopted here.

2.2 Rheometric tests

The rheological measurements of the silicone elastomer were carried out on a rheometric HAAKE MARS III (see Fig. 1a) that operates in a cone-and-plate geometry with a diameter of 35 mm and 2° angle, as shown in Fig. 1b. The temperature of the trays was controlled using a Peltier effect oven and a cooling pump. Shear viscosity measurements were carried out at different temperatures over the range of 25 to 100 °C and at 1 to 100 s^{-1} of shear rate. The values of the shear viscosity for the elastomer materials were determined using only component A without the catalyst.

2.3 Curing measurement

The curing measurement of the RTV silicone elastomers was carried out in dynamic mode using a rotational HAAKE MARS III rheometer operating in parallel-plate mode (see Fig. 1c). The trays had a diameter of 20 mm and a thickness of 0.5 mm. A force of 1 N was imposed when the measurement began whilst the resulting gap was maintained. The mixtures of different silicones were characterised for their cure characteristics using the mean of the torque curves obtained under isothermal conditions. The test temperatures used were from 25 to 100 °C. The rheometric measurements were imposed with a constant deformation (1%) and frequency (1 Hz). From the rheometer, the values of the torque, the storage modulus G' and the loss modulus G'' were obtained during the curing measurement. The storage modulus is the elastic solid like behaviour G' and the loss modulus is the viscous response G''. The complex shear modulus G^* is equal to the square root of the sum of G' squared and G'' squared. These will cross over when the frequency is equal to the reciprocal relaxation time. These data were used to calculate the cure kinetic parameters.

3 Rheokinetic models

3.1 Viscosity model

Various rheological models exist to describe the dependence of the viscosity on the shear rate $\dot{\gamma}$ and temperature T [22]. The power-law model, as expressed by Eq. (1), for viscosity is the following:

$$\eta(\dot{\gamma}, T) = \eta_0(T)\dot{\gamma}^{n-1} \tag{1}$$

where η_0 and n are, respectively, the zero-shear-rate viscosity and the power-law index. For a Newtonian fluid, the power-law index is equal to 1. For a shear-thinning fluid, the power-law index is between 0 and 1, and for a shear thickening fluid, it is greater than 1. The flow index, n, of the power-law

Table 1 Mechanical properties of the different RTV silicone elastomers used in this work

Materials	Density (g/cm^3)	Hardness Shore A	Tensile strength (MPa)	Elongation at break (%)	Mix ratio A:B	Preparation
M4370	1.43	55	3.0	130	9:1	Curing at room temperature
M4470	1.44	60	4.5	120	3% T37	
M4641	1.07	43	4.5	300	10:1	
M4670	1.28	55	5.5	250	10:1	

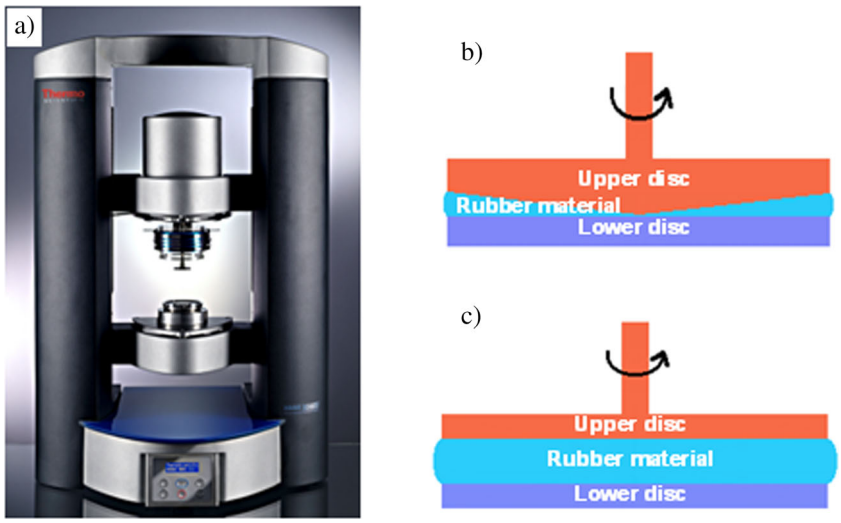

Fig. 1 **a** Rotational HAAKE MARS III rheometer. **b** Cone-and-plate geometry. **c** Plate-and-plate geometry

behaviour indicates the shear sensitivity. A smaller n of the polymer indicates a greater shear sensitivity and more pseudoplasticity. Some moulding defects are associated with small n, i.e. greater shear sensitivity.

Other models are frequently used to better fit the data over the entire shear rate range [23]. In the Carreau-Yasuda model, as expressed by Eq. (2), the viscosity is the following:

$$\eta(\dot{\gamma}, T) = \eta_0(T)\left(1 + \left(\lambda(T)\dot{\gamma}\right)^a\right)^{(n-1)/a} \tag{2}$$

where η_0, λ, a and n are the fitting parameters. More specifically, η_0 denotes the zero-shear-rate viscosity, the parameter λ is a constant with unit of time where its $\frac{1}{\lambda}$ is representing the shear rate at the transition from Newtonian to shear-thinning behaviour, a determines the width of the transition region between η_0 and the powder law region and n is the power-law index describing the slope of the viscosity curve with respect to shear rate in the shear-thinning region.

An Arrhenius-type relation was adopted to account for the temperature dependence for each kinetic parameter. The rheological model will be defined by the following equation:

$$\frac{\eta_0(T)}{\eta_0(T_0)} = \frac{\lambda(T)}{\lambda(T_0)} = \exp\left(\frac{E_a}{R}\left(\frac{1}{T} - \frac{1}{T_0}\right)\right) \tag{3}$$

where E_a, R and T_0 are, respectively, the activation energy, the universal gas constant (=8.134 J mol^{-1} K^{-1}) and the reference temperature. The activation energy of flow gives an indication about the molecular structure and chain branching.

3.2 Kinetic modelling

The cure kinetic parameters were defined using the proposed models by Claxton-Liska and Deng-Isayev, which are frequently used for the kinetic curing modelling of elastomers.

There are different definitions of the induction period or scorch time for elastomers [24]. Consideration of the induction period, which is due to curing, is necessary to prevent any vulcanisation reaction from taking place during the pouring stage of the casting process. In this study, the scorch time was defined as the time when the test began until the time when the values of the storage modulus G' and loss modulus G'' were the same.

The Claxton-Liska model [16] was used to fit the scorch time, as expressed by Eq. (4), which has an Arrhenius dependence on temperature, of the elastomer at different temperatures:

$$t_s = t_0 \exp\left(\frac{T_0}{T}\right) \tag{4}$$

where t_s is the scorch time, t_0 and T_0 are the material-dependent constants and T is the absolute temperature.

The state of a silicone elastomer during an isothermal vulcanisation reaction can be described by a cure degree α ranging from 0 (uncured) to 1 (complete reaction) [25]. Three steps are generally observed: an induction period, during which the modulus increases very slowly (α remains close to zero), followed by the cure step, with a sharp increase of the elastic modulus (and α). During this step, the modulus increases up to a maximum value $G'_{\max}$ [25]. The cure degree, which can be related to the heat released during the reaction due to the cross-linking of silicone elastomers, is an exothermic process [19].

From the cure data obtained from the rheometer curve, the cure degree α can be calculated using the following equation:

$$\alpha = \frac{M_t - M_L}{M_H - M_L} \tag{5}$$

where M_L, M_t and M_H are, respectively, the minimum torque, the torque at time t and the maximum torque.

Three variables establish the relationship between the cure degree, the time and the temperature (Eq. (6)). The model proposed by Deng-Isayev in [18], as expressed by Eq. (6), was used to determine the cure behaviour:

$$\alpha = \frac{k(t-t_s)^n}{1 + k(t-t_s)^n} \tag{6}$$

in which the parameter k is the rate constant and is expressed by an Arrhenius-type temperature dependence with the relation:

$$k = k_0 \exp\left(\frac{-E_0}{RT}\right) \tag{7}$$

where t, n, k_0, E_0 and R are, respectively, the time of the reaction, the order of reaction, the pre-exponential factor of the reaction velocity, the activation energy and the universal gas constant.

3.3 Fitting procedure

From the rheological measurement, the shear viscosities versus the shear rate and temperature curves were fitted using a power-law and Carreau-Yasuda models, where the fitting parameters were determined using the inverse method. In addition, the constants from the Claxton-Liska and Deng-Isayev models were obtained by data fitting techniques using the inverse method with the curve fitting software Origin from the curing measurement experimental data.

The different identifications using the inverse method have been achieved by solving a minimisation problem of the cost function, defined in Eq. (8), using algorithms based on the generalised reduced gradient method:

$$\min_x \| F(x,\ x_{\text{data}}) - y_{\text{data}} \|_2^2 = \min_x \sum_i \left(F(x,\ x_{\text{data}\ i} - y_{\text{data}\ i}) \right)^2 \tag{8}$$

where y_{data} is the experimental data curve and x_{data} is the estimated value of the rheological or vulcanisation behaviour models according to variable values of the model parameters being optimised. $F(x, x_{\text{data}})$ is the rheological or curing model used and x is the parameter to identify.

4 Results and discussions

4.1 Rheological results

Viscosity is an important parameter in the evolution of the rheological behaviour of silicone. Figure 2a–d shows the viscosity shear rate curves of silicone elastomers tested at

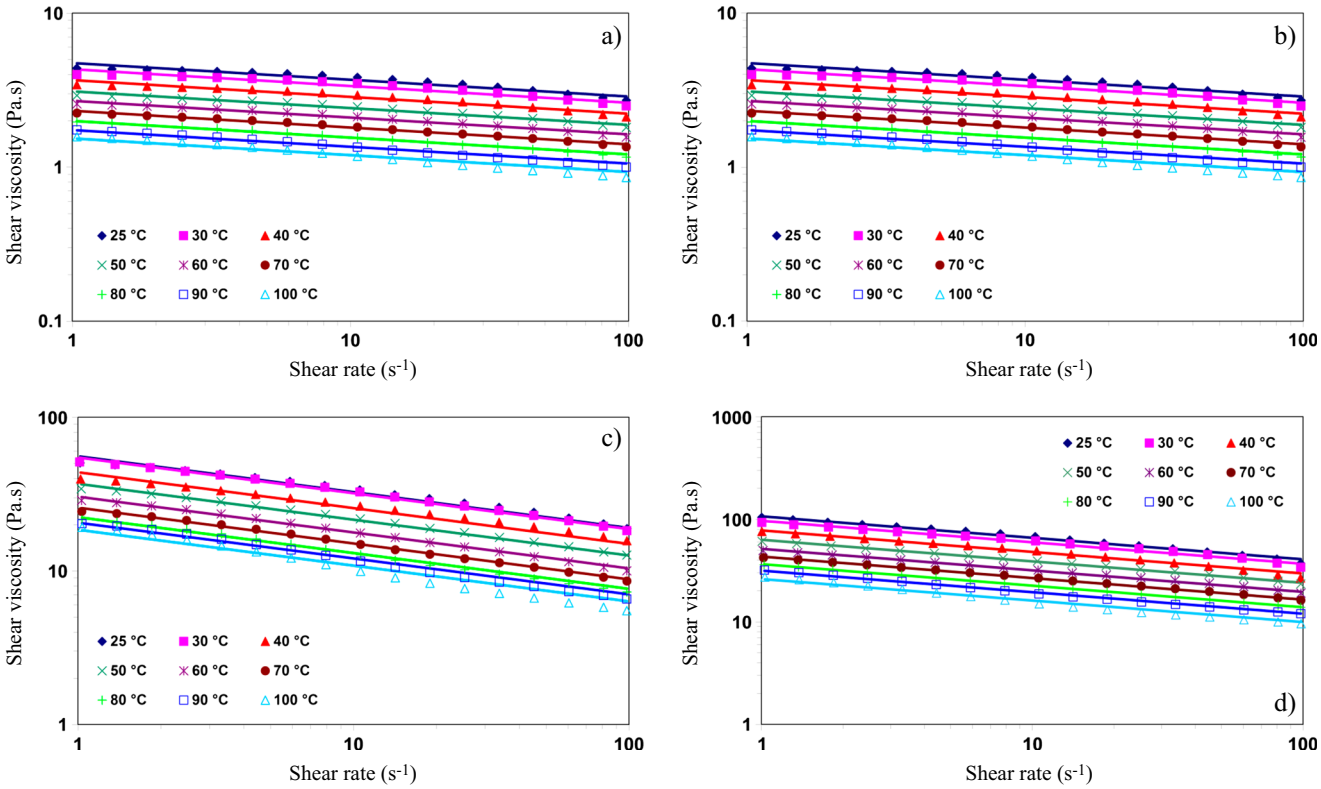

Fig. 2 Evolution of shear viscosity versus the shear rates at different temperatures for the experimental curves (*symbol*) and the identified power-law model (*solid line*) using different silicone elastomers. **a** M4370. **b** M4470. **c** M4641. **d** M4670

Table 2 Material constants for the power-law model obtained after identification

Materials	T_o (°C)	E_a (kJ/mol)	$\eta_0(T_o)$ (Pa s)	n
M4370	25	13.88	4.75	0.89
M4470	25	14.30	9.28	0.90
M4641	25	14.41	55.75	0.77
M4670	25	17.30	106.98	0.79

Table 3 Material constants for the Carreau-Yasuda model obtained after identification

Materials	T_o (°C)	E_a (kJ/mol)	$\eta_0(T_o)$ (Pa s)	$\lambda(T_o)$	a	N
M4370	25	13.90	7.44	0.11	1.07	0.80
M4470	25	14.30	8.91	0.26	1.14	0.86
M4641	25	14.47	67.82	0.58	1.14	0.74
M4670	25	17.30	178.29	1.46	1.25	0.78

different temperatures in the range of 25 to 100 °C. The silicone viscosity decreases with the shear rate and temperature, indicating pseudoplastic flow behaviour. One can also observe that the differences between the experimental curves at different temperatures are relatively small. Effectively, the rheological model prediction using the estimated parameters, which are plotted in Fig. 2, gives a qualitative description of the data.

The melts were obviously shear thinning and displayed a power-law behaviour. The power-law model was fitted to the experimental results using an Arrhenius-type temperature dependence. The reference temperature was selected to be 25 °C. The model parameter values resulting in the best fits to the experimental data for the power-law model and Arrhenius equation are listed in Table 2. The measured viscosity values and the corresponding fitted viscosity curves for all different silicone elastomers are given in Fig. 2a–d. For each tested material, a reasonable fit was obtained for the test temperatures over the shear rate ranges.

The shear viscosity decreased with an increase in the shear rate and temperature corresponding to pseudoplastic behaviour laws. The M4370 and M4470 elastomers have low shear viscosity, and the maximum shear rate of less than 6 Pa s was obtained at 100 °C and 1 s^{-1}, as shown in Fig. 2a, b. The M4641 and M4670 elastomers have greater viscosities than other elastomers (M4370 and M4470), and the maximum shear rates are, respectively, 50 and 100 Pa s obtained at 100 °C and 1 s^{-1}, as shown in Fig. 2c, d.

After curve fitting using the inverse method, the reactive viscosity model used to describe the rheological properties of

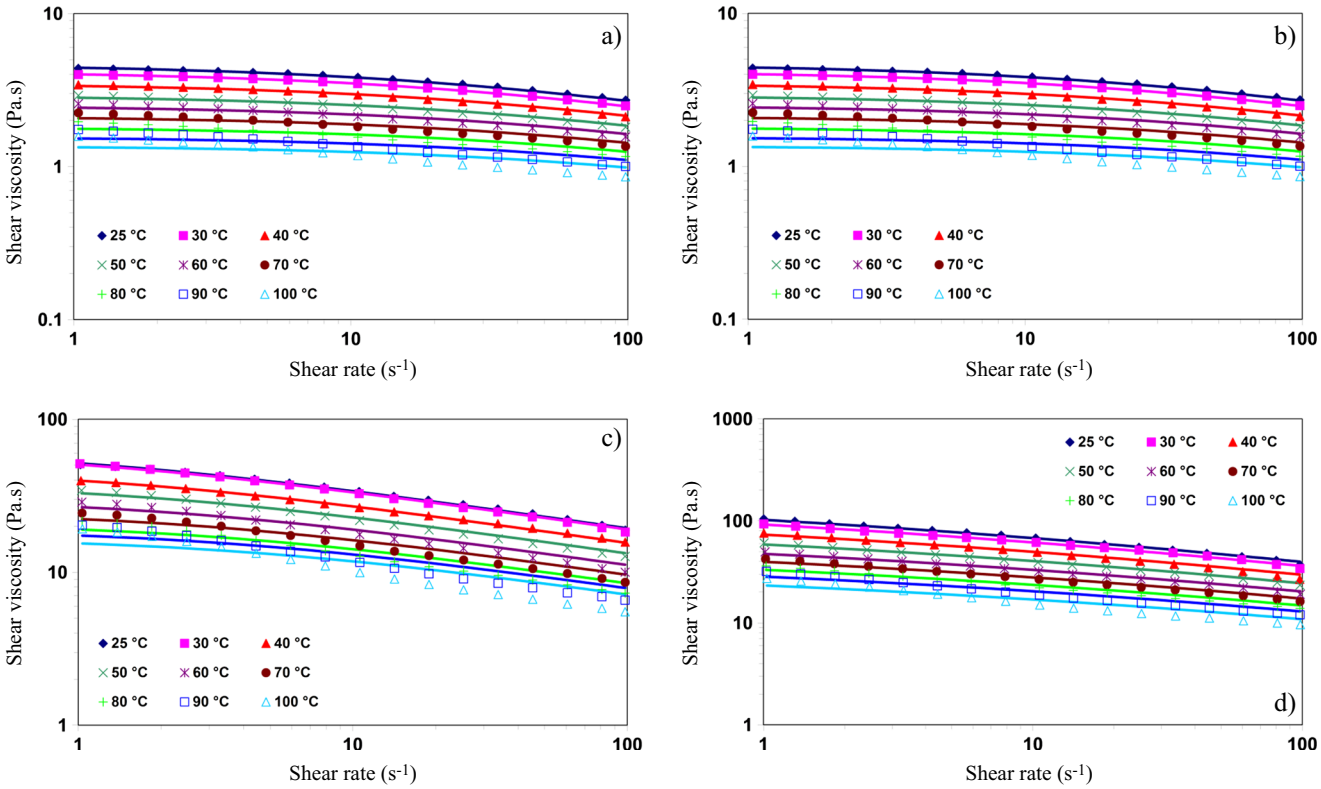

Fig. 3 Evolution of the shear viscosity versus the shear rate at different temperatures for the experimental curves (*symbol*) and the identified Carreau-Yasuda model (*solid line*) using different silicone elastomers. **a** M4370. **b** M4470. **c** M4641. **d** M4670

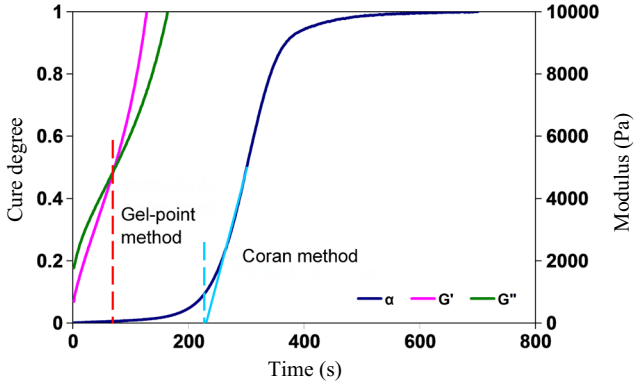

Fig. 4 Comparison of the point-gel and Coran methods to determine the induction times

different elastomers is given by the value of n and varies from 0.77 to 0.90, corresponding to a shear-thinning behaviour. The different values of the activation energy vary from 13.88 to 17.30 kJ mol^{-1}.

The Carreau-Yasuda model was fitted to the experimental results with an Arrhenius-type temperature dependence. The reference temperature selected was 25 °C. The model parameter values resulting in the best fit to the experimental data for the Carreau-Yasuda model and the Arrhenius equation are listed in Table 3. The measured viscosity values and the corresponding fitted viscosity curves for the different silicone elastomers are given in Fig. 3a–d. For each tested material, a reasonable fit was obtained for the lower temperatures over the shear rate ranges, and at higher temperatures, the Carreau-Yasuda model cannot reasonably fit the experimental results. This result is because, at high temperatures, the elastomer material has a shear-thinning behaviour over the shear rate ranges.

After curve fitting using the inverse method with the Carreau-Yasuda model, for different elastomers, the value of n varied from 0.74 to 0.86, corresponding to a shear-thinning behaviour. The various values of the activation energy varied from 13.90 to 17.30 kJ mol^{-1}. A comparison of n and E_a obtained after the identification of the two models (power-law and Carreau-Yasuda models) shows that the values are approximately the same.

Table 4 Material constants for the Claxton-Liska model obtained after identification

Elastomer	Coran method			Gel-point method		
	t_0 (s)	T_0 (K)	R^2	t_0 (s)	T_0 (K)	R^2
M4370	exp(−22.68)	9,357	0.9997	exp(−26.54)	10,303	0.9992
M4641	exp(−17.46)	7,882	0.9989	exp(−17.19)	7,627	0.9942
M4670	exp(−19.88)	8,855	0.9873	exp(−18.16)	8,036	0.9811

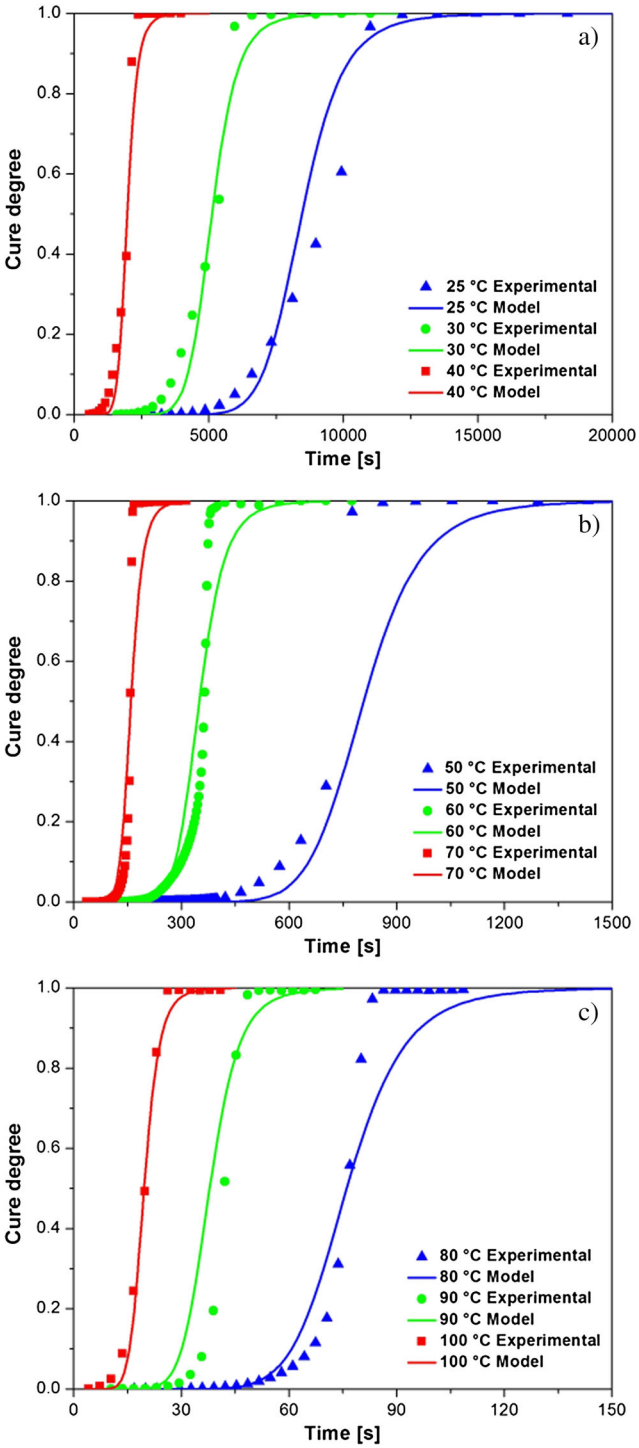

Fig. 5 Evolution of cross-linking versus time at different temperatures for the experimental curves (*symbol*) and the identified model (*solid line*) using the M4370 silicone elastomer. **a** 25–40 °C. **b** 50–70 °C. **c** 80–100 °C

4.2 Curing results

The cycle time is a very important parameter because a high cure time basically means lower profits. The cure time is the

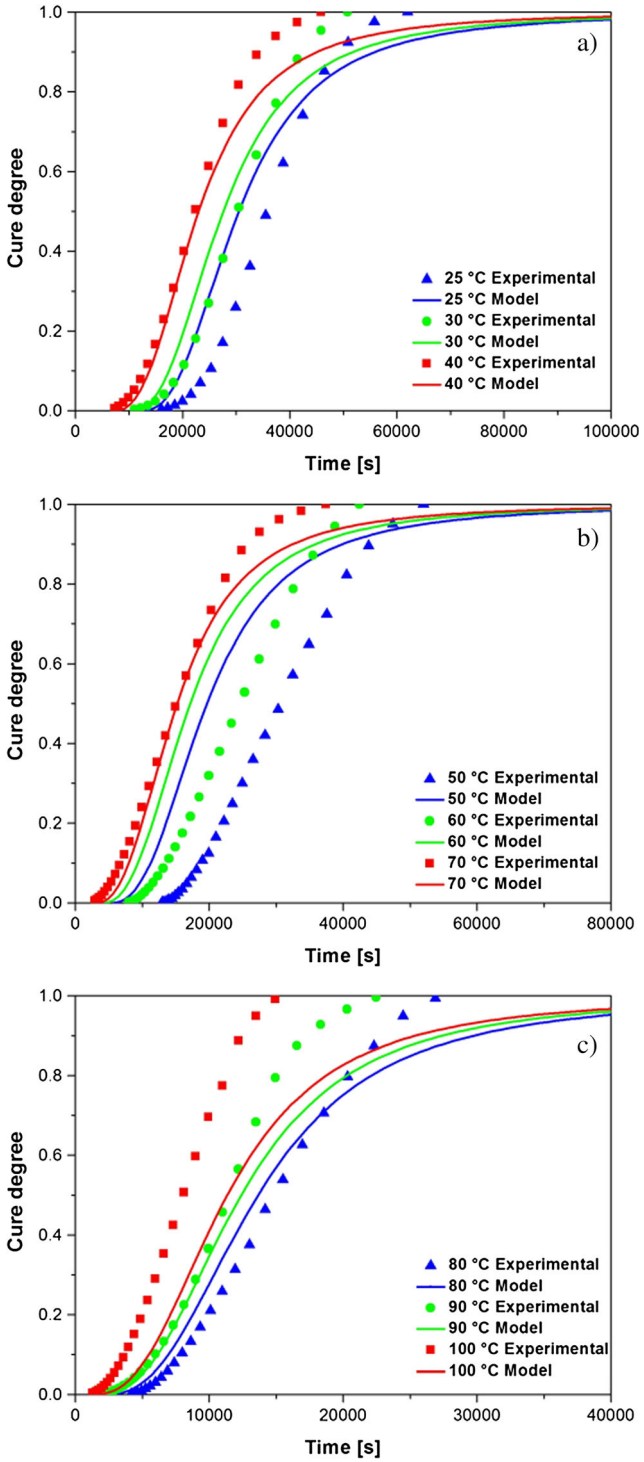

Fig. 6 Evolution of the cross-linking versus time at different temperatures for the experimental curves (*symbol*) and the identified model (*solid line*) using the M4470 silicone elastomer. **a** 25–40 °C. **b** 50–70 °C. **c** 80–100 °C

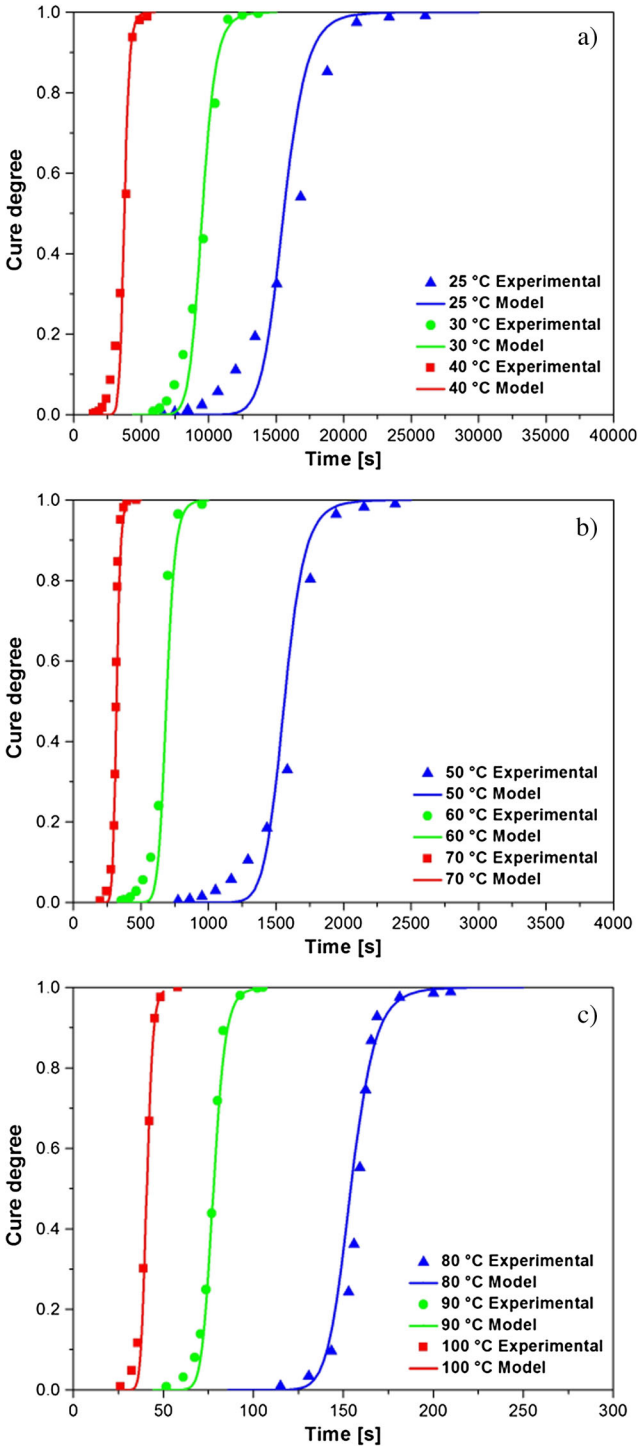

Fig. 7 Evolution of the cross-linking versus time at different temperatures for the experimental curves (*symbol*) and the identified model (*solid line*) using the M4641 silicone elastomer. **a** 25–40 °C. **b** 50–70 °C. **c** 80–100 °C

longest part of the cycle and is influenced by the choice of materials and their properties. A. Harkous et al. proposed some methodologies to determinate the gel-point value [26]. There studied at different temperatures to improve the understanding of the different cross-linking steps and to determine the best method which thermal or rheological characterisation

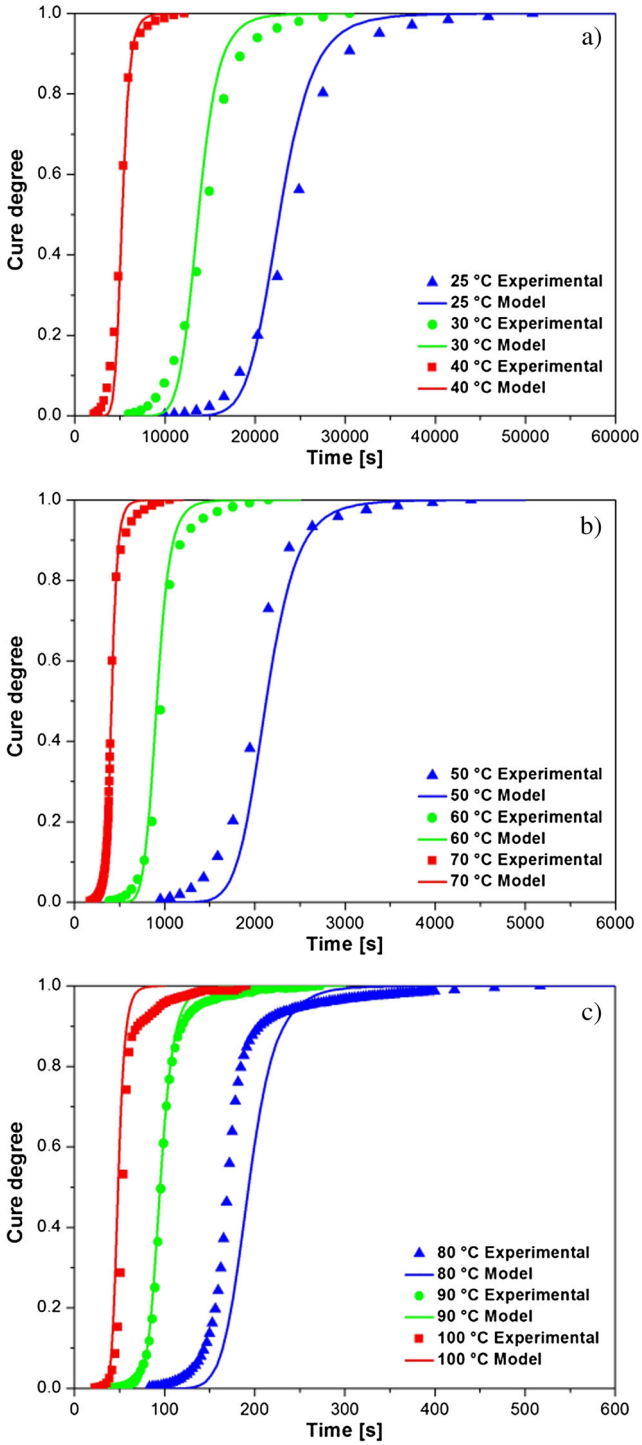

Fig. 8 Evolution of the cross-linking versus times at different temperatures for the experimental curves (*symbol*) and the identified model (*solid line*) using the M4670 silicone elastomer. **a** 25–40 °C. **b** 50–70 °C. **c** 80–100 °C

represents the reaction. There results show that the LSR network undergoes specific development during cross-linking.

The induction times at each test temperature for the various silicone elastomers were measured using two methods. The

Table 5 Material constants for the Deng-Isayev model obtained after identification

Materials	K_0 (s^{-1})	E_0 (kJ/mol)	n
M4370	exp(156.83)	552.62	7.62
M4470	exp(−17.19)	18.48	2.51
M4641	exp(230.07)	805.56	10.45
M4670	exp(155.52)	557.16	7.28

Coran methods are defined by the tangent of the cure curve with the horizontal time axis. The gel-point methods consist of determining the time when the storage modulus is equal to the loss modulus.

The scorch time has been determined using the inverse method in both methods (Coran and gel-point method) in terms of t_o and T_o, as seen in Fig. 4. It shows that the cure degree increases with increasing cure time and that the curves can be divided into three periods: induction, cure and reversion. During the induction period, the cure degree is nearly zero and increases slowly. Then, it grows rapidly toward one during the cure period. This *S*-shaped behaviour suggests that the reaction mechanism of vulcanisation could be described by simple kinetic models (see Fig. 4). After 600 s, the cure

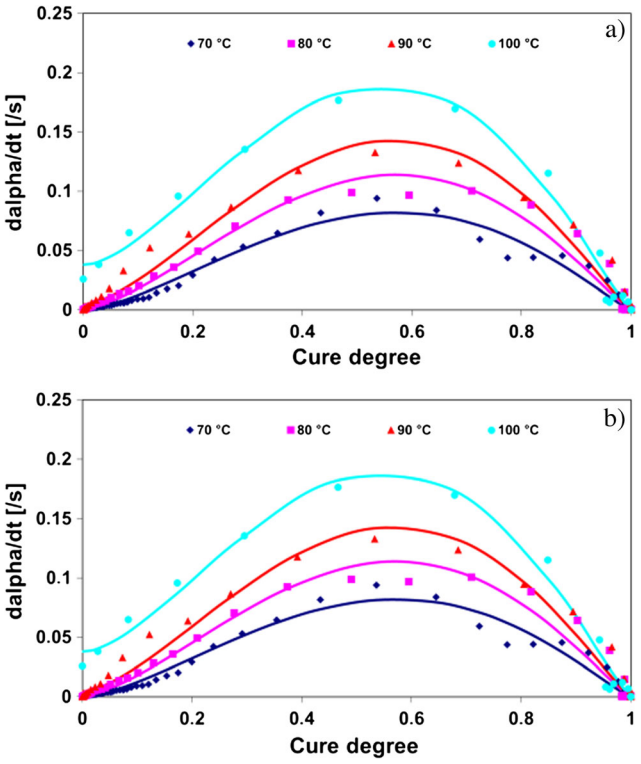

Fig. 9 Evolution of the cross-linking rate versus times **a** on the cross-linking **b** at different temperatures for the experimental curves (*symbol*) and the identified model (*solid line*) using the M4770 silicone elastomer from 70 to 100 °C

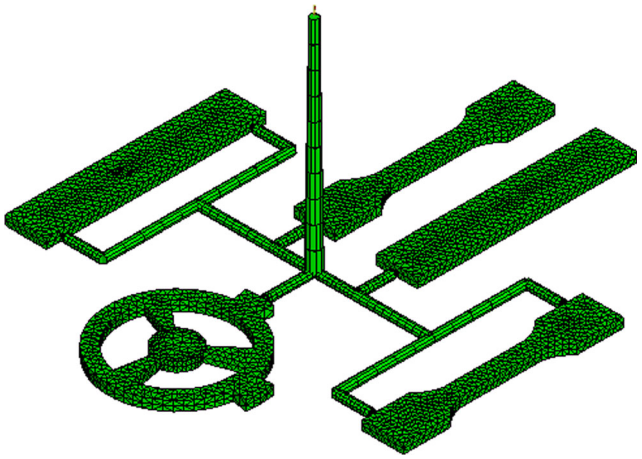

Fig. 10 Description of the mesh used in the thermoplastic injection moulding using the Cadflow software. **a** Mesh of the different die cavities used for elastomer injection moulding (3D tetrahedral elements, 4308 nodes, 11,114 elements)

degree reaches 1. At the beginning of the experiment, the values of G' and G'' increase slowly due to the growth of the molecule molar mass resulting from the condensation process and reveal the formation of cross-links between the molecules [26] (see Fig. 4). After some time, a cross-linking network appears throughout the sample. After a longer time, the cross-linking network continues to develop as shown by the increase in both modulus G' and G'' [26]. At 180 s, the values of G' and G'' is 10,000 Pa.

These data were fitted to the Claxton-Liska model by curve fitting using an inverse method in the Origin software, and fitting constant values together with the regression value are detailed in Table 4. The correlation R^2 value close to 1 proves that there was an efficient identification procedure for the values of t_o and T_o, as seen in Table 4. The induction times obtained from the curing measurement show a good fit to the Claxton-Liska model. In the second case, equivalent values of t_o and T_o were obtained. For example, after identification of the elastomer M4641 using the Coran and gel-point methods, T_0 was equal to 7882 and 7627 K and t_0 was equal to exp.(−17.46) and exp.(17.19), as seen in Table 4.

4.3 Fitting parameters

Experimental data with their respective fitting curves over the test temperature ranges for the silicone elastomers are shown in Figs. 5, 6, 7 and 8. The thermal curves present an earlier start of the reaction, and the degree of cure increases rapidly with increasing time and then gradually approaches 1, as shown in the lower part. The value is a function of time, and the cure process is faster as the temperature increases for each test temperature from 25 to 100 °C, as seen in Figs. 5, 6, 7 and 8. The temperature increase is faster for the compounded elastomer than for the cured elastomer. This results in the same cure versus time evolution for different RTV silicones (see Figs. 5, 6, 7 and 8).

Fig. 11 Numerical simulation results of the elastomer injection moulding; the evolution of the filling stage corresponds, respectively, to 0.01, 0.05, 0.13 and 0.27 s in **a**–**d** short shot filling states

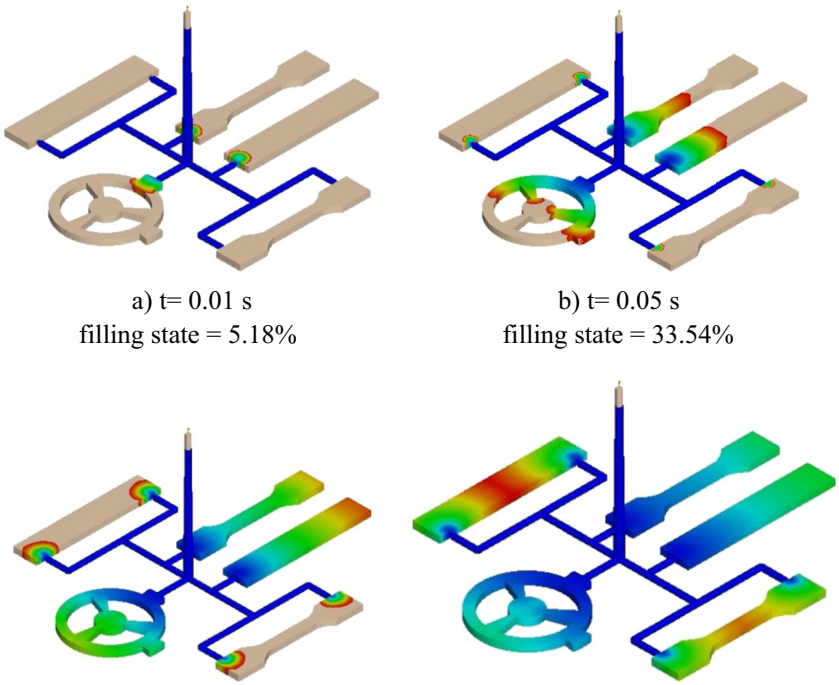

a) t= 0.01 s
filling state = 5.18%

b) t= 0.05 s
filling state = 33.54%

c) t= 0.13 s
filling state = 71.76%

d) t= 0.27 s
filling state = 99.96%

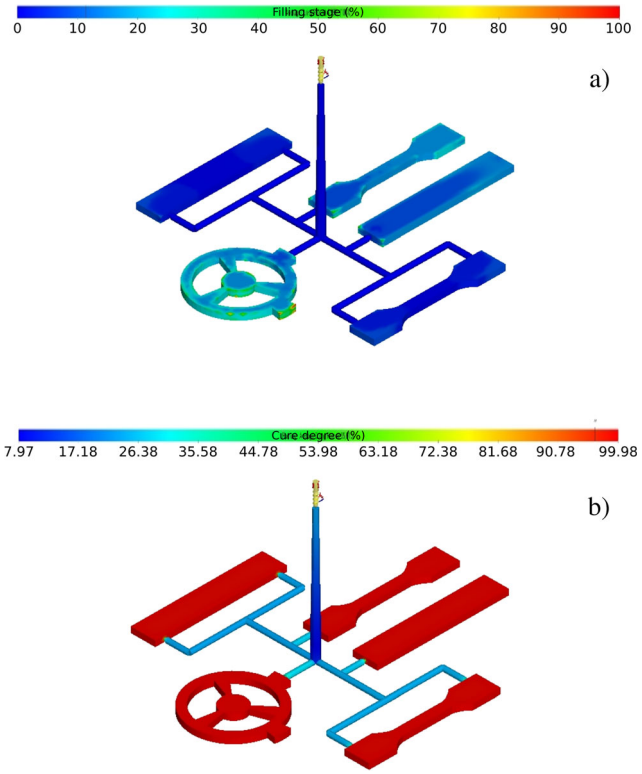

Fig. 12 Numerical simulation results of the elastomer injection moulding at the end of filling process. **a** Filling stage. **b** Temperature distribution

The comparison between the experimental and calculated cross-linking degrees using the Deng-Isayev's model is related to Table 5. The experimental results are greater than the calculated results for many temperatures. Despite this, the Deng-Isayev's model presents an accurate description of the silicone cross-linking.

For example, the full cure corresponding to M4670 silicone cross-linking has been obtained at a long cure time (500 s) at an imposed temperature of 80 °C and a short cure time (75 s) for a temperature equal to 100 °C, as seen in Fig. 8.

The fitting parameters for the different elastomeric compounds using the Deng-Isayev model are shown in Table 5. After curve fitting using the inverse method with the Deng-Isayev model, for different elastomers, the value of n varies from 2.51 to 10.45. The various values of the activation energy vary from 18.48 to 805.56 kJ mol^{-1}.

It appears that the variation of the necessary cure time for elastomeric materials demonstrates an exponential decrease as a function of temperature. In addition, the fitting curves were observed to be in better agreement with the experimental data for the M4370, M4641 and M4670 silicone elastomers, with a poorer agreement for M4470. This is because M4470 has less variation in the necessary cure time over the test temperature ranges and the duration of the curing measurement is not long enough to describe the curing perfectly.

After a certain transformation of the experimental data, the dependence of $\frac{\partial\alpha}{\partial t}$ on α was obtained (see the conditions in Fig. 9a, b). This figure clearly illustrates that all of the $\frac{\partial\alpha}{\partial t}$ curves remain approximately unchanged even when the reaction temperature changes, which is indicative of the autocatalytic reaction.

5 Numerical simulations and discussion

The 3D mesh of the various die cavities moulds were used in the finite element software Cadmould to simulate the elastomer injection moulding process of producing components having different tensile, bending and wheel test specimens, as illustrated in Fig. 10. In addition, simulation analyses require accurate rheological and kinetic properties to generate the best predictions [27]. It is important to provide accurate identification about rheokinetic models for elastomer silicones under the conditions encountered during processing so that the simulation software can work efficiently. The parameters identified using the rheokinetic behaviour laws have been implemented in the software for the different elastomers used for these studies (Tables 3 and 4). The injection parameters used for the simulation are the following: injection parameter equal to 10 MPa and mould temperature equal to 100 °C after the filling state.

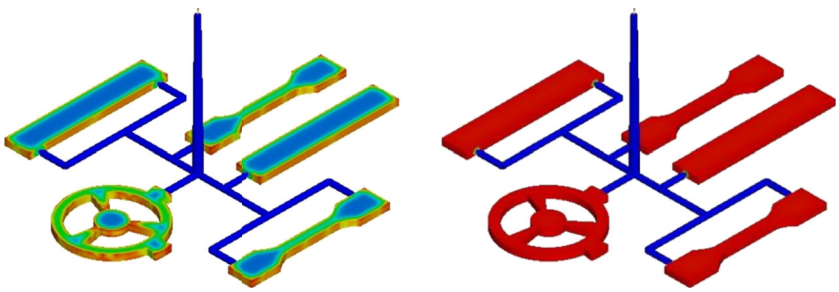

a) t= 25.44 s
Cure degree = 39.27%

b) t= 49.07 s
Cure degree = 99.92%

Fig. 13 Numerical simulation results of the cure degree at different filling stages (**a**, **b**)

The evolution of the filling stage from the beginning to the entire filling for the different die cavities is illustrated in Fig. 11a–d corresponding, respectively, to 0.01, 0.05, 0.13 and 0.27 s and filling state ratios of 5.18, 33.54, 71.76 and 99.96%.

The results of the elastomer injection moulding are illustrated at the end of the elastomer injection moulding in Fig. 12a, b with M4370. The entire filling of the die cavities was obtained without filling defects after 5 s, as seen in Fig. 12a. The cure degree during the injection moulding is also illustrated in Fig. 12b and begins with the reticulation of runners and gates after 7 s. This shows that cure degree at the end of the filling stage was almost zero and increases significantly during the heating stage. Moreover, the cure degree distribution demonstrates the effect of temperature for the cure kinetic reaction.

The evolution of the cure degree rate is illustrated at two different filling rates at 39.27 and 99.92% at 25.44 and 49.07 s, as seen in Fig. 13a, b, respectively. A faster cure kinetic reaction was also observed at the exterior surface.

6 Conclusion

In this work, the rheokinetic behaviours of different RTV silicone elastomer materials were investigated using a rotational rheometer. This study demonstrates the reliability of the experimental protocol. This protocol was applied to characteristic silicone elastomers with the aim of improving our understanding of the material behaviour during the elastomer injection process.

For the shear viscosity behaviour, the power-law model fits the rheological experimental data well over the test temperature ranges at low shear rates, and the Carreau-Yasuda model fits the low temperatures well. For the cure behaviour, the induction times and cure kinetic were modelled satisfactorily using the experimental data obtained from the rotational rheometer. The scorch time was defined as the time when the storage modulus was equal to the loss modulus. In addition, the scorch appears to be a function of temperature and fits the Claxton-Liska model well. Subsequently, the material constants were determined according to the Deng-Isayev model through the use of curve fitting and the inverse method. The kinetic results presented here confirm that the model describes the silicone cross-linking kinetics well. The shape of the model suits the description of cure degrees.

The rheokinetic material databases were used along with the Cadmould software to simulate the elastomer injection moulding process of different die cavity moulds. The results of the simulation predicted the mould filling and cure degree state into the die mould cavity when the flow and curing characteristics of silicone elastomers have been investigated properly and accurately.

However, the methods proposed in this study could well represent the overall experimental data for different silicone elastomers; thus, it could be readily employed for simulation of the elastomer injection moulding process. This type of model might also be suitable to predict the flow behaviour of other silicone elastomers if the appropriate material coefficients are selected.

$d\alpha/dt$, cure rate (s^{-1}); E_a, activation energy (J mol^{-1}); G, storage modulus (Pa); G'', loss modulus (Pa); G^*, complex shear modulus (Pa); k, k_0, temperature-dependent parameters according to Arrhenius law (s^{-1}); M_H, maximum torque (N m); M_L, minimum torque (N m); M_t, torque at time t (N m); R, universal gas constant (J mol^{-1} K^{-1}); T, temperature (°C; K); t, t_0, time (s); t_s, scorch time (s); T_0, temperature-independent constants (K); α, cure degree; η, viscosity (Pa s); η_0, zero-shear-rate viscosity (Pa s); $\dot{\gamma}$, shear rate (s^{-1}); η_0, n, λ, a, viscosity parameters (Pa s)

Acknowledgements Thanks to the support of the collaborative FUI LSR Silicone Project and of all our partners. Thanks to the Bluestar Silicones for their positive and fast answer to all our requirements.

Compliance with ethical standards

Conflict of interest The authors declare that they have no conflict of interest.

References

1. Jerschow P (2001) Silicone elastomers, Wacker-Chemie GmbH, Rapra review reports. Report 137 12:5
2. Tang Y, Tan WK, Fuh JYH, Loh HT, Wong YS, Thian SCH, Lu L (2007) Micro-mould fabrication for a micro-gear via vacuum casting. J Mater Process Technol 192-193:334–339
3. Chung S, Park S, Lee I, Jeong H, Cho D (2004) A study on microreplication of real 3D-shape structures using elastomeric mold: from pure epoxy to composite based on epoxy. Journal of Machine Tools & Manufacture 44:147–154
4. Sahli M, Gelin J-C, Barriere T (2015) Replication of microchannel structures in WC–Co feedstock using elastomeric replica moulds by hot embossing process. Mater Sci Eng C 55:252–266
5. Ye X, Liu H, Ding Y, Li H, Lu B (2009) Research on the cast molding process for high quality PDMS molds. Microelectron Eng 86:310–313
6. Galeotti F, Chiusa I, Morello L, Gianì S, Breviario D, Hatz S, Damin F, Chiari M, Bolognesi A (2009) Breath figures-mediated microprinting allows for versatile applications in molecular biology. Eur Polym J 45:3027–3034
7. Bernardi L, Hopf R, Ferrari A, Ehret AE, Mazza E (2017) On the large strain deformation behavior of silicone-based elastomers for biomedical applications. Polym Test 58:189–198
8. Bernardi L, Hopf R, Sibilio D, Ferrari A, Ehret AE, Mazza E (2017) On the cyclic deformation behavior, fracture properties and cytotoxicity of silicone-based elastomers for biomedical applications. Polym Test 60:117–123
9. Arrillaga A, Zaldua AM, Atxurra RM, Farid AS (2007) Techniques used for determining cure kinetics of rubber compounds. Eur Polym J 43:4783–4799

10. Hong IK, Lee S (2013) Cure kinetics and modeling the reaction of silicone rubber. Journal of Indusrial and Engineering Chemistry 19: 42–47
11. Polgar LM, Kingma A, Roelfs M, van Essen M, van Duin M, Picchioni F (2017) Kinetics of cross-linking and de-cross-linking of EPM rubber with thermoreversible Diels-Alder chemistry. Eur Polym J 90:150–161
12. Bideau PL, Ploteau JP, Dutournié P, Glouannec P (2009) Experimental and modelling study of superficial elastomer vulcanization by short wave infrared radiation. Int J Therm Sci 48:573–582
13. Khang TH, Ariff ZM (2012) Vulcanization kinetics study of natural rubber compounds having different formulation variables. J Therm Anal Calorim 109:1545–1533
14. Wang J, Fang X, Wu M, He X, Liu W, Shen X (2011) Synthesis, curing kinetics and thermal properties of bisphenol-AP-based benzoxazine. Eur Polym J 47:2158–2168
15. Erfanian M-R, Anbarsooz M, Moghiman M (2016) A three dimensional simulation of a rubber curing process considering variable order of reaction. Appl Math Model 40:8592–8604
16. Claxton WE, Liska JW (1964) Calculation of state of cure in rubber under variable time-temperature conditions. Rubber Age 95(2):237
17. Kamal MR, Sourour S (1973) Kinetics and thermal characterisation of thermoset cure. Polym Eng Sci 13(1):59
18. Isayev AI, Deng JS (1988) Non isothermal vulcanisation of rubber compounds. Rubber Chem Technol 61(2):340
19. In-Kwon H, Sangmook L (2013) Cure kinetics and modeling the reaction of silicone rubber. J Ind Eng Chem 19:42–47
20. Isayev AI, Deng JS (1987) Non isothermal vulcanisation of rubber compounds. ACS Rubber Division Meeting, Montreal
21. Sykutera D, Bielinski M (2010) The use of injection moulding process simulation software Cadmould for injection mould designing. J Pol CIMAC 5:207–213
22. White JL (1992) Rheological behaviour and boundary condition characteristics of rubber compounds. Journal of Applied Polymer Science: Applied Polymer Symposium 50:109–132
23. Bird RB, Armstrong RC, Hassager O (1987) Dynamic of polymeric liquids, volume 1: fluid mechanics, secon edn. Wiley, New York
24. Marzocca AJ, Mansilla MA (2006) Vulcanization kinetic of styrene-butadiene rubber by sulfur/TBBS. J Appl Polym Sci 101: 35–41
25. Leroy E, Souid A, Sarda A, Deterre R (2013) A knowledge based approach for elastomer cure kinetic parameters estimation. Polym Test 32:9–14
26. Harkous A, Colomines G, Leroy E, Mousseau P, Deterre R (2016) The kinetic behavior of liquid silicone rubber: a comparison between thermal and rheological approaches based on gel point determination. React Funct Polym 101:20–27
27. Khang TH, Ariff ZM (2014) Mold filling simulation dependence on material data input for injection molding process of natural rubber compound, Carl Hanser Verlag GmbH & Co. KG, International Polymer Processing. J Polym Process Soc 325, 331